

This is a repository copy of Shape vs flow: a 2D statistical shape analysis of the projection of common iliac veins in patients with deep vein thrombosis.

White Rose Research Online URL for this paper: https://eprints.whiterose.ac.uk/id/eprint/233275/

Version: Accepted Version

Proceedings Paper:

Otta, M. orcid.org/0000-0002-8062-1354, Zajac, K. orcid.org/0000-0003-1393-8236, Malawski, M. orcid.org/0000-0001-6005-0243 et al. (4 more authors) (2025) Shape vs flow: a 2D statistical shape analysis of the projection of common iliac veins in patients with deep vein thrombosis. In: Wachinger, C., Luijten, G., Elhabian, S., Gopinath, K. and Egger, J., (eds.) UNSPECIFIED Shape in Medical Imaging (ShapeMI 2025), 23-27 Sep 2025, Daejeon, South Korea. Lecture Notes in Computer Science, 16171. Springer Nature Switzerland, pp. 292-303. ISBN: 9783032067739. ISSN: 0302-9743. EISSN: 1611-3349.

https://doi.org/10.1007/978-3-032-06774-6_22

© 2025 The Authors. Except as otherwise noted, this author-accepted version of a paper published in Shape in Medical Imaging is made available via the University of Sheffield Research Publications and Copyright Policy under the terms of the Creative Commons Attribution 4.0 International License (CC-BY 4.0), which permits unrestricted use, distribution and reproduction in any medium, provided the original work is properly cited. To view a copy of this licence, visit http://creativecommons.org/licenses/by/4.0/

Reuse

This article is distributed under the terms of the Creative Commons Attribution (CC BY) licence. This licence allows you to distribute, remix, tweak, and build upon the work, even commercially, as long as you credit the authors for the original work. More information and the full terms of the licence here: https://creativecommons.org/licenses/

Takedown

If you consider content in White Rose Research Online to be in breach of UK law, please notify us by emailing eprints@whiterose.ac.uk including the URL of the record and the reason for the withdrawal request.



Shape vs flow: a 2D statistical shape analysis of the projection of common iliac veins in patients with deep vein thrombosis

 $\begin{array}{c} {\rm Magdalena~Otta^{\star1,2,3[0000-0002-8062-1354]},~Karol~Zając^{1[0000-0003-1393-8236]},} \\ {\rm Maciej~Malawski^{1,6[0000-0001-6005-0243]},~Ian~Halliday^{2,3},~Chung~Lim^{5},~Janice~Tsui^{4,5},~and~Andrew~Narracott^{2,3[0000-0002-3068-6192]} \end{array}$

- Sano Centre for Computational Medicine, Kraków, Poland (https://sano.science/)
- ² Division of Clinical Medicine and Population Health, University of Sheffield, Sheffield, UK
- ³ Insigneo Institute for *in silico* medicine, University of Sheffield, Sheffield, UK
 ⁴ University College London, London, UK
 - ⁵ Royal Free London NHS Foundation Trust, London, UK
- ⁶ Faculty of Computer Science, AGH University of Kraków, Kraków, Poland

Abstract. Deep vein thrombosis (DVT) of the lower limb is characterised by the formation of abnormal blood clots in deep veins of lower extremity. Changes in blood flow have been associated with an increased risk of thrombus development. Understanding the relationship between variable venous anatomy and haemodynamics can reveal insights to support clinical decision-making processes. The purpose of this study was to combine statistical shape modelling (SSM) - to analyse venous shape - and computational fluid dynamics (CFD) - to estimate blood flow in the common iliac vein to demonstrate the feasibility of a combined framework to support the treatment of DVT. Principal geodesic analysis was used to extract dominant shape modes from a set of 24 venous shapes in 2D: 8 patient-specific extracted from standard angiograms and 16 synthetic complementing the set. Steady-state CFD simulations were run on the associated 3D geometries. Low wall shear stress distributions below three thresholds (< 0.15, < 0.10, < 0.05Pa) were the haemodynamic risk metrics of choice. The distribution of CFD output metrics was evaluated using the three most dominant shape modes from PGA and compared to the three modes that showed the strongest correlation with the CFD metrics, illustrating that they are not the same. The study demonstrated the feasibility of combining SSM and CFD to examine the importance of shape variability and inflow in a local region of the venous circulation. It will serve as a basis for extended work on a larger set of venous shapes extracted from standard medical images.

Keywords: statistical shape modelling \cdot computational fluid dynamics \cdot deep vein thrombosis

^{*} Corresponding author: m.otta@sanoscience.org

1 Introduction

Deep vein thrombosis (DVT) of the lower extremity is a condition of pathological clots that form in the deep veins of the leg, often in the iliofemoral region where it is also the most symptomatic and most likely to cause long-term complications known as post-thrombotic syndrome (PTS). PTS affects up to 50% of patients with DVT and 30% are at risk of recurrent DVT within a decade of diagnosis [1]. Understanding the relationship between variable venous anatomy and haemodynamics could provide new information to optimise current clinical decisionmaking, which is largely based on available images, the most common being 2D angiography. 3D volumetric images are not collected after invasive treatment in standard clinical practice [2]. Changes in blood flow, especially prolonged residence, have been associated with adverse biological responses leading to the development of blood clots, but flow is currently not measured in the clinic. Blood flow in various segments of the circulatory system can be modelled using the well-established method of computational fluid dynamics (CFD) [3]. Statistical shape modelling (SSM), on the other hand, is an established technique for analysing complex anatomical shapes, building statistical models from available data, such as medical images. Among others, it allows us to predict the shape of anatomical structures and analyse their deformations [4]. This work focuses on building a pipeline that integrates statistical shape modelling (SSM) with computational fluid dynamics (CFD) to explore the relationship between vascular morphology and haemodynamics. Traditional shape analysis does not incorporate blood flow information. However, haemodynamic metrics could potentially provide valuable risk predictions for patients with venous thrombosis.

In this study, for SSM, 2D venous shapes are used, extracted from angiography images showing projections of the common iliac veins in patients after DVT treatment. The shapes are then used to construct 3D representations assuming that there is no out-of-plane curvature. The relative importance of shape and boundary conditions is also evaluated. The approach has the potential to identify shape biomarkers predictive of adverse haemodynamics. It builds on previous combinations of SSM and CFD approaches that have been reported in the literature. These include the evaluation of haemodynamics, in both the aortic valve region [5], and throughout the 3D anatomy of the aorta [6]. To our knowledge, such techniques have not been applied to examine the variability in the anatomy of the venous system, which is the focus of this computational workflow which serves as a proof-of-concept of the methodology in this domain. Understanding how variations in the anatomical shape of veins influence haemodynamics could support risk assessment and treatment planning for patients with DVT and PTS.

2 Methods

Our methodology follows the workflow presented in Fig. 1. A set of 2D venous shapes was constructed as a mix of patient-specific geometries (from angiography images) and synthetic geometries to enhance shape variability and improve

statistical robustness. All geometries were pre-processed to ensure consistent topology and alignment. The set was used to perform a statistical shape analysis with a principal geodesic analysis using Deformetrica [7]. 3D representations of the 2D shapes were constructed in the form of STL meshes to run the CFD analysis. The goal was to investigate how the shape of the vessels correlates with the flow characteristics and how much information about haemodynamics could be extracted from the 2D vein projections.

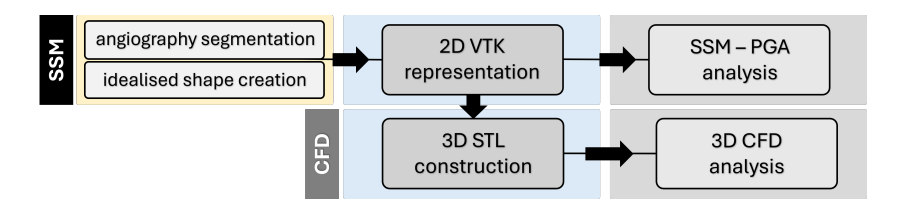


Fig. 1. Flowchart overviewing the methodology applied in this research from segmentation of medical images through appropriate 2D and 3D formats to statistical shape analysis and 3D CFD simulations.

2.1 Angiography segmentation and idealised shape creation

This study used 2D angiography images from eight patients treated for DVT with stents in the common iliac vein. The images represent a 2D projection of the considered vein. A custom Python tool extracted the contours of the vessel placing points along the visible walls and computed the centreline of the vein (Fig. 2). All lines were interpolated to a fixed number of points, and the radius of the vessel was estimated at 25 locations using distances from the centreline to the walls. In the absence of information on the resolution of the angiography images, pixel scaling was based on a ruler visible in the image. To supplement the dataset, 16 idealised 2D geometries were created, including several with an increasing degree of curvature (denoted C_i), an increasing degree of stenosis (denoted S_i) and both (denoted C_i). The complete set of the 24 2D venous shapes used in the shape analysis is shown in Fig. 3.

2.2 Shape preparation for SSM

All 2D shapes were saved in VTK format as polyline objects with the same number of defining points orientated clockwise to ensure point correspondence between shapes. A legacy VTK format was used to ensure compatibility with Deformetrica v4.3, the statistical shape modelling tool used here [8]. To avoid the algorithm that interprets the differences in position and scale of the shapes as meaningful deformations, all shapes were translated to the common origin and normalised in scale using the available functionality of Deformetrica framework.

4 M. Otta et al.

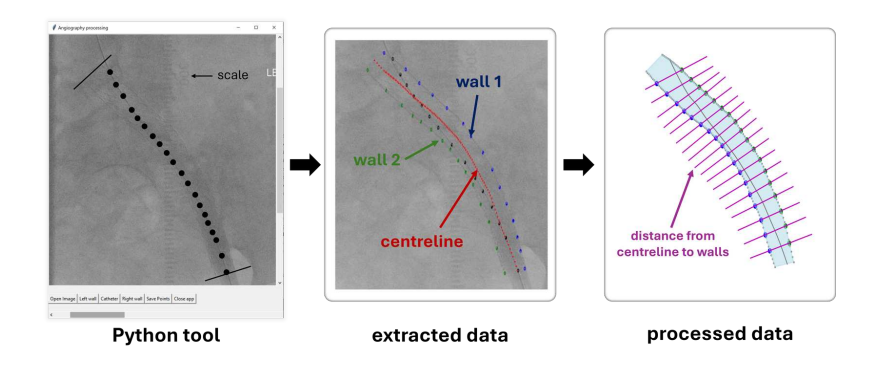


Fig. 2. Extraction of the contour of the common iliac vein projection from angiography images with custom Python code.

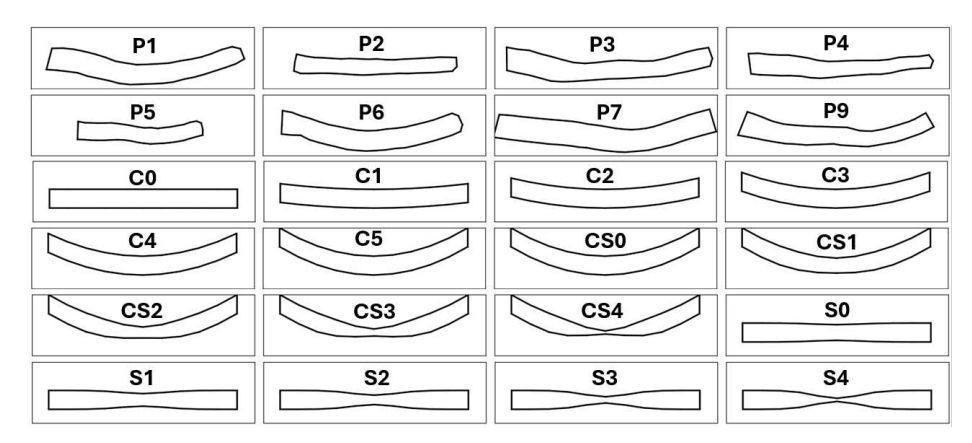


Fig. 3. A complete set of the 24 venous shapes of the common iliac in 2D, 8 extracted from angiography images (top 2 rows) and 16 synthetic shapes with variable curvature and stenosis.

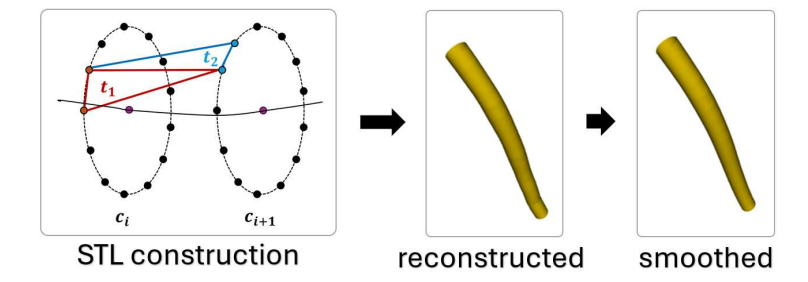


Fig. 4. The process of constructing an STL surface for a single vessel. Triangles are formed iteratively between contours c_i and c_{i+1} (left). The surface representation of the vein is constructed and smoothed out (right).

2.3 Construction of 3D geometries for CFD

A three-dimensional representation of the common iliac vein was constructed around the computed centrelines. Estimates of the cross sections were constructed using radii computed from the angiograms and known radii in surrogate shapes at a number of locations along the centrelines. A Python script was written to create a triangulated surface in STL format that can be further processed for CFD simulations. The script includes ordering points, defining each cross section, and interpolating them to the same fixed number of points. It iterates through the contours, taking two points from the contour c_i and one point from c_{i+1} to construct a triangle, then taking two points from c_{i+1} and one from c_i . For each i^{th} contour, the points are iterated in order and the contour c_{i+1} is first rotated to minimise the twist of the constructed triangles between c_i and c_{i+1} (Fig. 4). The normal vectors of each triangle were computed by taking the cross product of two vectors that form the edges of a given triangle. After initial surface mesh construction, surface meshes of different veins were further processed in SpaceClaim 2024 R2 and prepared for Ansys Fluent simulations.

2.4 Shape modelling

Deformetrica v4.3 [7] was used to carry out the statistical shape modelling process with two frameworks: Deterministic Atlas (DA) and Principal Geodesic Analysis (PGA). A theory behind Deformetrica's applications is summarised in Refs. [8] and [9]. Software documentation is available in Ref. [10]. The DA model estimates a template shape that is a form of average configuration across the considered data set that accounts for complex deformations. It also provides a set of control points that cover the space spanned by the shapes and guide the deformation. The information on how the template shape can be deformed to obtain each of the shapes in the data set is encoded as momenta, representing vectors at the control points. The primary use of DA was to compute the mean venous shape (template) for further use in the PGA. A template was chosen from a converged analysis with good-quality shape reconstructions. PGA is a generalised form of Principal Component Analysis (PCA). Instead of linear components, it identifies geodesics, which are the shortest paths on a curved space, that best explain the variability in a set of shapes. PGA computes the principal geodesics, the directions of maximal variance, around the template shape. Similarly to DA, it returns a template shape and a set of control points used. These can be supplied prior to analysis; otherwise, the software computes a sensible set on its own. Momenta explaining the deviations of each shape from the template are also returned. During the analysis, each shape is projected into a latent space which describes how each subject deviates from the template along the principal geodesics. PGA returns coordinates for a chosen number of latent dimensions. Ten shapes generated by moving along each principal direction in steps of standard deviations σ are also returned - five in the negative direction $(-5\sigma, -4\sigma,$..., -1σ) and five in the positive $(+1\sigma, +2\sigma, ..., +5\sigma)$. In short, principal directions are the directions in the latent space that capture the most variation in the

data set. In this analysis, we computed 15 latent dimensions (also referred to as modes of shape variation). The first modes are typically the most dominant such that mode 1 captures the most shape variation, mode 2 second most, orthogonal to mode 1, next mode 3, orthogonal to both mode 1 and 2 and so on. The first three modes should explain the majority of the variance; however, it is sensible to verify the contribution of every computed mode.

2.5 Setup of CFD simulations

3D representations of the venous shapes were run through an ANSYS Fluent 2024 R2 workflow from meshing to output analysis. A polyhedral mesh with the element size of 0.0002m was created for every 3D shape based on a mesh sensitivity analysis. The steady-state simulations, assuming laminar flow, were initialised with constant zero pressure at the outlet and parabolic inlet flow estimated from previous work [11] at 0.0782m/s. In addition, the inflow velocity was varied by $\pm 20\%$ to provide an assessment of the relative importance of variation in the shape and in the model boundary conditions (inflow). Blood was assumed to be incompressible and Newtonian with constant density $\rho = 1050 kgm^{-3}$ and viscosity $\mu = 0.0035 Pa \cdot s$. Meshes created with custom Python code were prepared for simulation in SpaceClaim 2024 R2. The CFD workflow in ANSYS Fluent 2024 R2 was automated using the PyFluent library, for both meshing and simulations with a batch processing approach. The effect of shape variation and changes in boundary conditions on local haemodynamics was assessed by calculating the surface area of the vessel wall subjected to low wall shear stress, WSS (Fig. 5) below three threshold values: ≤ 0.15 Pa (navy blue), ≤ 0.10 Pa (blue), and < 0.05 Pa (magenta). Low WSS is considered related to blood coagulation and clot formation [12].



Fig. 5. Low wall shear stress distribution on a geometry P1, reconstructed from patient data. Extracted metrics of interest are the surface area values subject to WSS below three thresholds.

2.6 Combination of shape and flow metrics

The latent coordinates of the PGA were linked to the corresponding CFD metrics. The relationships were visualised for the three most dominant shape modes and simple statistical analysis explored the correlations between shape variation and haemodynamic output. The three shape modes most correlated with the CFD metrics were visualised. Physiological interpretability entails the extent to which each mode captures the anatomical variation that affects blood

flow. Although dominant shape modes describe large-scale shape changes, less prominent ones may represent subtle features with significant impact on flow behaviour. Understanding this relationship helps link shape analysis to functional outcomes and improves the relevance of CFD-based predictions.

3 Results

This section reviews and compares the results of SSM and CFD analysis.

3.1 CFD outputs

Contour plots that demonstrate the variability in the low WSS area obtained in the CFD simulations are shown at the top of Fig. 6 for four geometries; a histogram that reports the size of the low WSS regions for all the geometries considered is shown at the bottom. Patient-specific geometries consistently show larger areas of low WSS compared to surrogate shapes. Among the surrogate shapes, those representing stenosis results in the largest areas of low WSS and indicate the possibility of more complex flow. The curvature surrogate geometries show the smallest areas, with shapes C0 - C4, not having WSS below 0.15Pa.

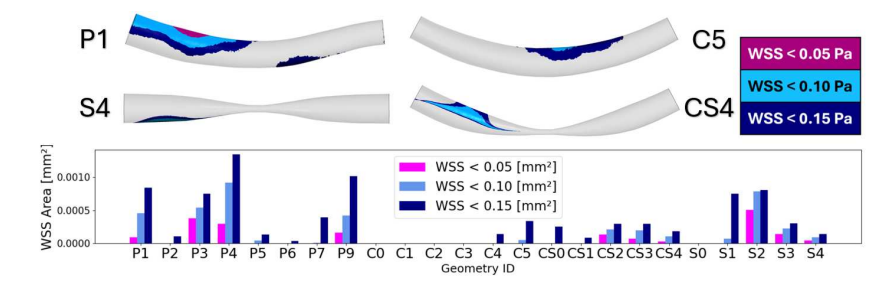


Fig. 6. Top: Examples of WSS outputs for different venous geometries, including patient-specific P1, curvature C5, stenosis S4 and a combination of curvature and stenosis CS4. **Bottom:** WSS areas for three considered thresholds across the data set.

3.2 Shape vs flow

Each shape considered is represented as a point in the latent shape space. Fig. 7 shows the distribution of shapes in the subspace defined by the three most dominant PGA modes. Columns correspond to different WSS thresholds, and rows correspond to inlet velocities. The intensity of the colour reflects the WSS area in $[mm^2]$, with variations indicating differences in magnitude between the applied conditions. Inlet velocity appears to have a minor effect, and no clear relationship is observed between the shape and the WSS outputs for the dominant modes in this preliminary setup, which used a single vein and simplified 2D to 3D geometry.

A simple correlation (Spearman) was calculated between the latent dimension coordinates and the WSS outputs. The three most significant (i.e., most correlated) modes for each output were identified (regardless of the direction of correlation), as shown in Fig. 8. These are not the same across the WSS outputs. For WSS < 0.05Pa, modes 6, 3 and 4 (as identified during shape analysis) are the most dominant, for WSS < 0.10Pa, modes 6, 3 and 4 and for WSS < 0.15Pa, modes 6, 11 and 12. If shape modes that dominate geometry also governed the CFD outcomes, the rankings in Fig. 8 would match the shape ranking, but it does not. This highlights a key aspect: modes that explain the most geometric variance are not necessarily the most influential for fluid dynamics. Dominant shape modes capture broad morphological trends, but may miss subtle features, while less prominent ones that fine-tune geometry can disproportionately affect haemodynamic metrics. This emphasises the importance of context-specific mode selection when linking shape models to CFD.

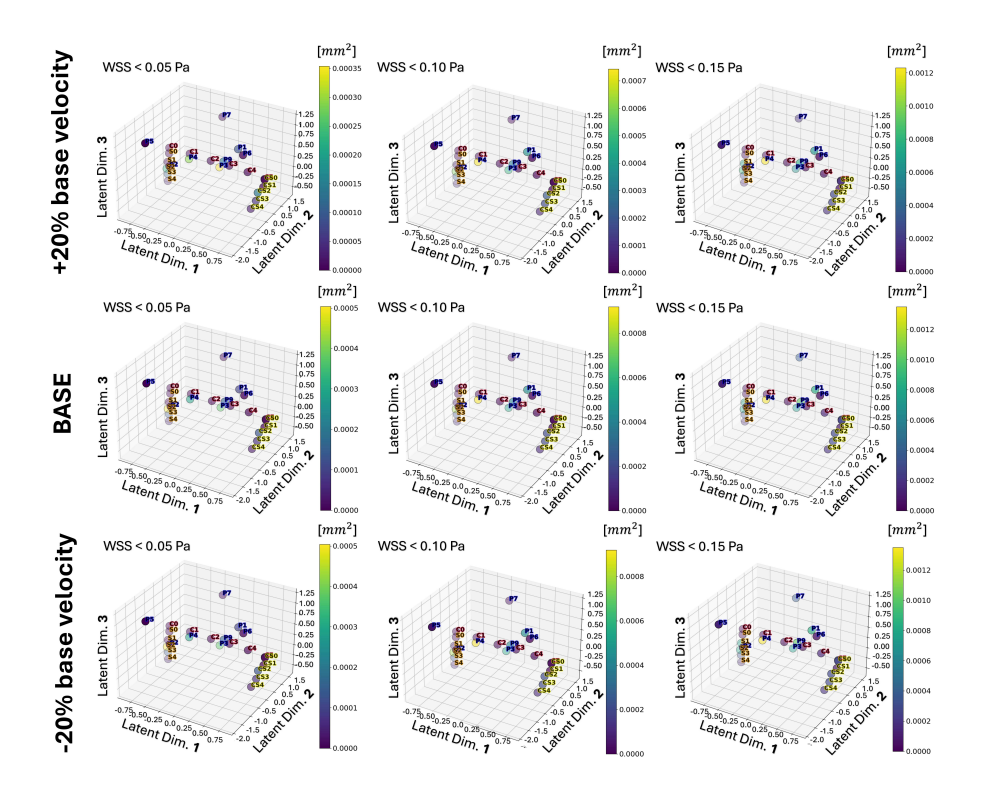


Fig. 7. Distributions of shapes in the latent space of three most dominant shape modes identified in the shape analysis. Dots are labelled by their shape IDs. The colour of the dots represents different CFD output metrics (one threshold value per column) for the base inlet velocity (middle row), velocity increased by 20% (top row), and decreased by 20% (bottom row). Labels refer to geometries in the set: patient-specific in blue, curved in red, stenosed in orange and both curved and stenosed in yellow.

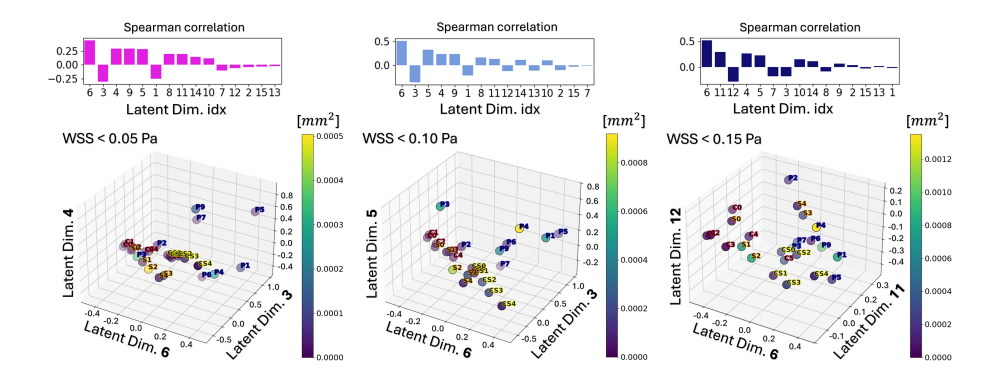


Fig. 8. Top: Histogram showing correlation between WSS area and latent coordinate for all latent dimensions (x-axis) for each of the WSS threshold values. Bottom: Distributions of shapes in the latent space for the three most correlated latent dimensions with each WSS metric. Labels refer to geometries in the set: patient-specific in blue, curved in red, stenosed in orange and both curved and stenosed in yellow.

4 Discussion

The study demonstrates the feasibility of combining shape analysis and CFD simulation to examine the importance of shape variability and inflow in a local region of the venous circulation, following DVT treatment.

This preliminary study used a small number of patient-specific geometries, with synthetic shapes added to increase the variability of the set. Although useful for exploring haemodynamic variation, synthetic shapes may not fully reflect anatomical or pathological diversity. Some shaes were highly exaggerated, particularly stenosed cases, potentially violating laminar flow assumptions and affecting CFD accuracy. The selection of shapes was driven by shape analysis rather than physiological realism, which means that extreme cases such as S4 may not represent the true haemodynamics of the patient. Future work will include a larger and more representative cohort of patients.

A set of 2D shapes was used for the SSM analysis framework and their simplified 3D representations were used to run the CFD analysis. This was dictated by the typical clinical workflow during DVT interventions, where 2D angiograms are available after treatment. In principle, the workflow used here can be readily extended to consider full 3D characterisations of vessel anatomy which could be provided with modifications to clinical workflows, e.g. acquisition of volumetric imaging such as MRI or CT post-intervention. A limitation of using 2D contours extruded in 3D geometries is that this approach neglects out-of-plane curvature, which can significantly influence local flow patterns and wall shear stress distribution. By simplifying the geometry of the vessel in this way, important anatomical features can be lost, potentially reducing the accuracy and physiological relevance of the CFD predictions. Furthermore, the study was based on a single vein rather than a unified model of multiple venous segments, which

limits generalisability and may overlook interactions between adjacent anatomical regions. These constraints mean that the findings should be interpreted as indicative rather than definitive, pending validation with full 3D models and broader anatomical datasets.

CFD simulations are based on assumptions such as steady-state flow, rigid walls, Newtonian blood flow, and idealised boundary conditions. These simplifications may affect the accuracy of haemodynamic metrics. Dynamic changes in shape (e.g., due to cardiac and respiratory cycles) and flow were not considered.

We have shown how latent shape dimensions correlate with derived flow characteristics. 15 latent shapes were computed with the PGA analysis; here, we have contrasted the distribution of CFD output metrics using the three most dominant modes from PGA and the three modes that correlate more significantly with the CFD metrics, showing that these are not the same. Ultimately, this surrogate approach could allow rapid estimation of haemodynamic risk metrics (through PGA alone), based on an established library of pre-computed CFD metrics, and has the potential to be delivered during the interventional procedure. Future work involving larger cohorts will explore the use of regression and machine learning models to identify relationships between anatomical shape modes and haemodynamic metrics such as wall shear stress and pressure distribution. Using shape modes as input features and CFD-derived metrics as predictive targets, these models will help determine which shape variations are most indicative of flow behaviour. This data-driven approach is expected to improve the detection of physiologically relevant shape patterns and support generalisation across diverse anatomical geometries.

Although PGA offers a compact representation of shape variability, interpreting individual modes in physiological or clinical terms remains challenging. More work is needed to explore how WSS thresholds relate to biological responses, such as thrombus formation. The framework presented here supports this by allowing for analysis across multiple thresholds and assessing their impact on output metrics. Ultimately, this approach holds promise for future translational applications, including patient-specific risk assessment based on haemodynamics.

5 Conclusion

The purpose of this analysis was to demonstrate the feasibility of a framework to integrate CFD-derived metrics (e.g., vessel areas subject to low wall shear stress) with shape descriptors to support the haemodynamic-based risk assessment for patients treated for DVT. This has been shown using 2D imaging data from angiography and has the potential to be extended to full 3D vessel anatomy. Future work will focus on applying this approach to a larger cohort of patients.

Acknowledgments. This project has received funding from the European Union's Horizon 2020 research and innovation programme under grant agreement No 857533. The publication was created within the project of the Minister of Science and Higher Education "Support for the activity of Centers of Excellence established in Poland under Horizon 2020" on the basis of the contract number MEiN/2023/DIR/3796 and

is supported by Sano project carried out within the International Research Agendas programme of the Foundation for Polish Science, co-financed by the European Union under the European Regional Development Fund. The authors acknowledge the Polish high-performance computing infrastructure PLGrid (HPC Center: ACK Cyfronet AGH) for providing computer facilities and support within computational grant no. PLG/2024/017108. This research was funded in whole or in part by National Science Centre, Poland 2023/49/N/ST6/04252.

Disclosure of Interests. The authors declare no potential conflict of interest.

Data access: https://doi.org/10.71580/sano/R3RRTZ

References

- 1. Baldwin, M.J. et al.: Post-thrombotic syndrome: a clinical review. Journal of Thrombosis and Haemostasis, **2**(11), 795-805 (2013), (https://doi.org/10.1111/jth.12180)
- 2. Kakkos, S.K. $_{
 m et}$ al.: Guidelines on the Management of Venous Thrombosis. Eur J Vasc Endovasc Surg., **2**(61), (2021),(https://doi.org/10.1016/j.ejvs.2020.09.023)
- Morris, P.D. et al.: Computational fluid dynamics modelling in cardiovascular medicine. Heart, 2(102), 18-28 (2016), (https://doi.org/10.1136/heartjnl-2015-308044)
- 4. Zhang, M., Golland, P., Statistical shape analysis: From landmarks to diffeomorphisms, Medical Image Analysis **33**, 155-158 (2016), (https://doi.org/10.1016/j.media.2016.06.025)
- Hoeijmakers, M.J.M.M., Waechter-Stehle, I., Weese, J., Van de Vosse, F.N., Combining statistical shape modeling, CFD, and meta-modeling to approximate the patient-specific pressure-drop across the aortic valve in real-time, International Journal for Numerical Methods in Biomedical Engineering, 36(10): e3387 (2020), (https://doi.org/10.1002/cnm.3387)
- 6. Pajaziti, E. et al., Shape-driven deep neural networks for fast acquisition of aortic 3D pressure and velocity flow fields, PLoS Computational Biology **19**(4): e1011055 (2023), (https://doi.org/10.1371/journal.pcbi.1011055)
- 7. Deformetrica (Version 4.3.0) [Computer software]. Aramis Lab. Available at: http://www.deformetrica.org
- 8. Bône, A., Louis, M., Martin, B., Durrleman, S. (2018). Deformetrica 4: An Open-Source Software for Statistical Shape Analysis. (https://doi.org/10.1007/978-3-030-04747-4 1).
- 9. Durrleman, S., Prastawa, M., Charon, N., Korenberg, J.R., Joshi, S., et al. Morphometry of anatomical shape complexes with dense deformations and sparse parameters. NeuroImage (2014), (https://doi.org/10.1016/j.neuroimage.2014.06.043)
- 10. Deformetrica. Documentation. Aramis Lab. Available at: https://gitlab.com/icm-institute/aramislab/deformetrica/-/wikis/home#introduction
- 11. Otta, M. et al. Towards sensitivity analysis: 3D venous modelling in the lower limb. in press, Accepted for ICCS 2025.
- 12. Mukul S.G. and Scott L.D.: Adhesion of normal erythrocytes at depressed venous shear rates to activated neutrophils, activated platelets, and fibrin polymerized from plasma. Blood **100**(10): 3797–3803 (2002), (https://doi.org/10.1182/blood-2002-03-0712)